Audio Engineering Society
Convention Paper 7997
Presented at the 128th Convention
2010 May 22–25 London, UK

Modeling Distortion Effects in Class-D Amplifier Filter Inductors

Arnold Knott[1], Tore Stegenborg-Andersen [1], Ole C. Thomsen [1], Dominik Bortis [2], Johann W. Kolar [2]
Gerhard Pfaffinger[3] and Michael A.E. Andersen[1]

[1] *Technical University of Denmark, 2800 Kgs. Lyngby, Denmark*

[2] *ETH Zurich / Power Electronics System Laboratory, CH-8092 Zurich, Switzerland*

[3] *Harman/Becker Automotive Systems GmbH, 94315 Straubing, Germany*

Correspondence should be addressed to Arnold Knott (`akn@elektro.dtu.dk`)

ABSTRACT

Distortion is generally accepted as a quantifier to judge the quality of audio power amplifiers. In switch-mode power amplifiers various mechanisms influence this performance measure. After giving an overview of those, this paper focuses on the particular effect of the nonlinearity of the output filter components on the audio performance. While the physical reasons for both, the capacitor and the inductor induced distortion are given, the practical in depth demonstration is done for the inductor only. This includes measuring the inductors performance, modeling through fitting and resulting into simulation models. The fitted models achieve distortion values between 0.03 % and 0.2 % as a basis to enable the design of a 200 W amplifier.

1. INTRODUCTION

Even other measures, like intermodulation distortion are more in depth measures, a distortion figure is the fundamental starting point to distinguish amplifiers. It reveals the noise level of the amplifier and provides the basics for more advanced tests as described in [1]. As the desired figures necessitate the precision of signal levels to be in the μV range, it makes sense to break the origin of the distortion mechanisms down into the various parts of an amplifier. For linear audio power amplifiers this was done in [2]. For the more efficient switch-mode audio power amplifiers a number of publications covered these mechanisms. The different stages of these amplifiers can be broken down according to the block diagram in figure 1.

The blocks and their distortion sources are:

Fig. 1 Block diagram of a switch-mode audio power amplifier

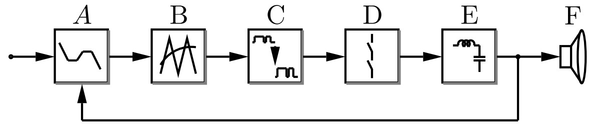

A. **Input and Control** The distortion is dominated in the input stage and regulator by either the used operational amplifier for time-continuous inputs and specified in their datasheets or, for time-discrete inputs, by the sampling process [3, 4, 5] or clock induced noise level [6].

B. **Modulator** The modulator induced distortion is mainly based on linearity of the carrier [7].

C. **Level Shifter** The impact of the level shifter on the audio performance has not been researched up to now and leaves room for further research.

D. **Power Stage** The power stages influence on the audio performance has been described in [8].

E. **Output Filter** This paper is dealing with the influence of the output filters properties on linearity of the amplifier.

F. **Loudspeaker** The transducers influence on audio performance has been described in [9] and broken down into single mechanisms in [10]

2. OUTPUT FILTER

The output filter is required to suppress the energy, which is used to operate the output stage in an efficient mode. The frequency of this energy is beyond the audible frequency range [11] and generally causing trouble in electromagnetic compatibility. The insertion of the filter is solving those, however generating audible effects and losses, which leads to the tradeoffs visualized in figure 2.

A simplified circuit diagram of the output filter is shown in figure 3 and its transfer function is given in 2.1 where V_{ps} denotes the output voltage of the power stage and V_{out} the output voltage of the amplifier, which is applied across the speaker terminals.

Fig. 2 Tradeoffs in output filter design.

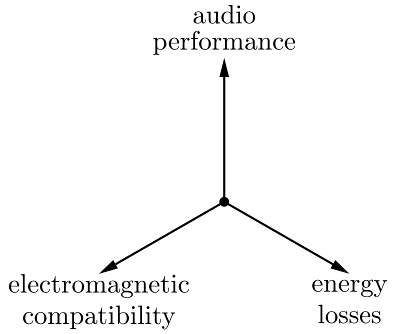

Fig. 3 Circuit of an output filter for an audio power amplifier.

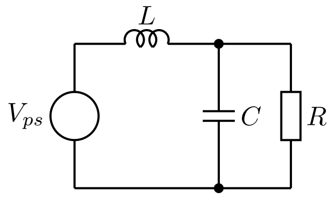

Equation 2.1 Transfer function of filter in figure 3.

$$\underline{H}\left(\underline{s}\right) = \frac{\underline{V}_{out}}{\underline{V}_{ps}} = \frac{1}{1 + \underline{s}\frac{L}{R} + \underline{s}^2 LC}$$

This paper is specifically investigating the nature and impact of the output filter on the audio performance. Therefore both filter components, the capacitors and the inductors physical properties are investigated in this section.

2.1. Capacitor

Capacitance C is defined as stored charge q per voltage V 2.2.

Equation 2.2 Definition of capacitance.

$$C = \frac{q}{V}$$

Applying Gauss Law to the charge allows itemization into electrical field $\vec{E}$ with vacuum permittivity ε_0 and displacement vector $\vec{P}$ via charge density ϱ and electric displacement $\vec{D}$ 2.3.

Equation 2.3 Gauss Law.

$$q = \iiint \varrho\, \delta Vol = \oint_A \vec{D}\, \delta\vec{s} = \oint_A \left(\varepsilon_0 \vec{E} + \vec{P}\right)\, \delta\vec{s}$$

The denominator of 2.2 can be expressed by Faradys law 2.4.

Equation 2.4 Farradays Law.

$$V = \oint_s \vec{E}\, \delta\vec{s}$$

Through both of those physical principles, the definition of capacitance can be rewritten as in 2.5

Equation 2.5 Definition of capacitance taking Gauss and Farradays Law into account.

$$C = \underbrace{\frac{\oint_A \varepsilon_0 \vec{E}\, \delta\vec{s}}{\oint_s \vec{E}\, \delta\vec{s}}}_{\text{linear part}} + \underbrace{\frac{\oint_A \vec{P}\, \delta\vec{s}}{\oint_s \vec{E}\, \delta\vec{s}}}_{\substack{\text{polarization}\\ \text{dependent}}}$$

The nonlinearity of the capacitor is therefore originated in the polarization defined through the electric susceptibility χ 2.6 for anisotropic dielectric materials [12].

Equation 2.6 Linear and nonlinear parts of displacement vector.

$$\frac{\vec{P}}{\epsilon_0} = \underbrace{\sum_j \chi_{ij}^{(1)} \vec{E}_j}_{\substack{\text{linear}\\ \text{suscepti-}\\ \text{bility}}} + \underbrace{\sum_{jk} \chi_{ijk}^{(2)} \vec{E}_j \vec{E}_k}_{\substack{\text{Pockels}\\ \text{Effect}}} + \underbrace{\sum_{jkl} \chi_{ijkl}^{(3)} \vec{E}_j \vec{E}_k \vec{E}_l}_{\text{Kerr Effect}}$$

This reveals the Pockels effect to be responsible for second order nonlinearities and the Kerr Effect to be the reason for third order effects.
For ferroelectric materials, the description of nonlinearity is getting somewhat more complicated, as the displacement vector has a hysteretic dependency on the electrical field. Theses hysteretic curves have been shown quantitativelty in [13].

2.2. Inductor

The equivalent physical derivation of the reasons for the nonlinearity of the inductor start with the definition of inductance 2.7 in dependency on magnetic flux Φ and electrical current I.

Equation 2.7 Definition of inductance.

$$L = \frac{\phi}{I}$$

Through Gauss Law of Magnetism Φ is expressed in 2.8 as a function of magnetic field $\vec{H}$ and the magnetization $\vec{M}$ with the aid of the permeability in vacuum via the magnetic flux density $\vec{B}$.

Equation 2.8 Gauss Law of Magnetism.

$$\Phi = \oint_S \vec{B}\, \delta\vec{A} = \oint_S \mu_0 \left(\vec{H} + \vec{M}\right)\, \delta\vec{A}$$

Through Amperes Circuit Law the current is expressed as a function of the magnetic field $\vec{H}$ as in 2.9.

Equation 2.9 Amperes Circuit Law.

$$I = \oint_C \vec{H}\, \delta\vec{l}$$

Taking both of those two laws into account, the definition of the inductance is rewritten in 2.10.

Equation 2.10 Definition of inductance taking Gauss and Amperes Law into account.

$$L = \underbrace{\frac{\oint\limits_S \mu_0 \vec{H}\,\delta\vec{A}}{\oint\limits_C \vec{H}\,\delta\vec{l}}}_{\text{linear part}} + \underbrace{\frac{\oint\limits_S \mu_0 \vec{M}\,\delta\vec{A}}{\oint\limits_C \vec{H}\,\delta\vec{l}}}_{\substack{\text{polarization}\\ \text{dependent}}}$$

The polarization dependent part $\vec{M}$ is not following the BH-curve, which has been numerically fitted in [14], but rather the Rayleigh Loop [15] which has been extended to symmetry of the loop as only limitation, by [16] as described in [17]. While the current I is linear dependent on the magnetic field $\vec{H}$, its relation to the magnetic polarization $\vec{M}$ contains higher order terms. This nonlinear dependency of magnetization on the magnetic field is covered by the high order terms in 2.11 by the named references.

Equation 2.11 Peterson relation.

$$\vec{M} = \chi\vec{H} + \mu_0 a_{11}\vec{H}^2 + \mu_0\left(a_{12} + a_{30}\right)\vec{H}$$

The coefficients a_{11}, a_{12} and a_{30} are the first Peterson Coefficients, describing both, the nonlinearity of the magnetization curve and ensure the fulfillment of the energy conservation law. As shown in [17] the lost energy in the magnetic field corresponds with the hysteresis losses in the material. Also in [17] the Peterson Coefficients got used to quantitatively describe the nonlinearity of the magnetic flux density for single sinusoidal tones as well as double sinusoidal tones and their intermodulation products.
For the choice of output filter inductors for switch-mode power amplifiers those coefficients are of quantitative interest. However the Peterson Coefficients where derived for small field excitations only, whereas the linearity of an amplifier is affected by the large signal behaviour of the magnetization loop. Therefore the next logical step is to measure the large signal behaviour of inductors and use the quantized data for estimation of the impact on the audio performance. This is done in the next section.

3. MODELING

Section 2 showed the duality between capacitor and inductor in theory. Consequently the rest of the paper is dealing with one of them only, without loosing generality for the other one. It is the inductor, which is generally dominating size constraints, electromagnetic compatibility challenges and showing the most interesting saturation effects. Therefore the inductors linearity is pursued furtheron in this paper.
Through the desired power rating of an amplifier and neglect of the ripple current, the current rating of the filter inductor is given. For the following analysis of inductors, a power rating of 200 W into a 4 Ω transducer is arbitrarily chosen. This leads to a peak current of 10 A through the filter inductor. Only few technical documentations of suitable components give the dependency of inductance on the current flowing through the windings like in [18]. Therefore a measurement setup is described following, allowing to derive this curve.

3.1. Measurement Setup

To measure the linearity of the inductor, it needs to be biased with the desirable current and simultaneously measured with an impedance analyzer. If an analyzer with current bias option is not available the bias can be done externally as shown in figure 4.
Through the inductor L_{inject} the device under test

Fig. 4 Measurement Setup.

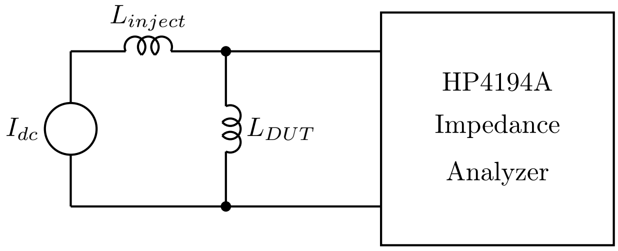

L_{DUT} is biased to the desired current level. To prevent damage on the gain phase analyzer, which is both superimposing the test signal as well as taking the measurement data, the voltage limitation of the current source shall be set below the maximum input rating of the analyzer. Otherwise a voltage leading to destruction in the input of the analyzer might occur in case the DUT fails. The purpose of the injection inductance is, to provide a high ohmic path for the measurement signal. Therefore the injection inductance needs to be significantly bigger than the inductance of the DUT. Also the injection inductance needs to be more linear than the device under test. This results into a high volume consuming inductor compared to the DUT. The parameters of the injection inductor are given in table 1.

Three possible output filter inductors have been chosen based on their rating. Their main parameters are compared in table 2. The inductance curves have been captured with the above described measurement method and the results are visualized in figure 5. The inductance droop varies from less than 1 %, around 3 % up to nearly 10 % with respect to the unbiased inductance measurement.

These relative variations shall not be confused with the distortion of an amplifier. The fitting of the inductance droop to a distortion number is done in the following section.

Table 1 Design of injection inductor.

core	air gap	turns	L_{inject}
ETD59-N97	1.6 mm	32	306 µH

Table 2 Parameters of the three devices under test.

	DUT-A	DUT-B	DUT-C
nominal inductance	22 µH	10 µH	10 µH
current rating	11 A	10 A	10 A
DC resistance	11 mΩ	8.8 mΩ	17.2 mΩ
resonant frequency	9.3 MHz	41 MHz	20 MHz
boxed volume	9.2 cm^3	1.6 cm^3	2.3 cm^3
footprint area	2.3 cm^2	1.9 cm^2	3.3 cm^2
datasheet	[19]	[20]	[21]

3.2. Fitting

Through the above shown nonlinear behaviour of the inductor, equation 2.1 is getting another dependency on the inductor current as shown in 3.1.

Fig. 5 Inductance curves.

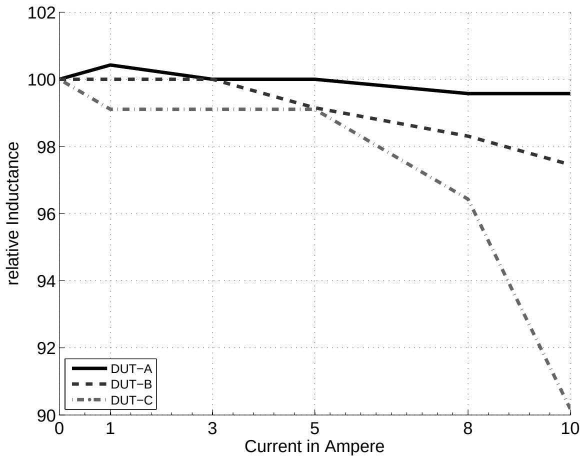

Equation 3.1 Transfer function taking nonlinearity of inductor into account.

$$\underline{H}\left(\underline{s}, \underline{I}_L\right) = \frac{\underline{V}_{out}}{\underline{V}_{ps}} = \frac{1}{1 + \underline{s}\frac{L\left(\underline{I}_L\right)}{R} + \underline{s}^2 L\left(\underline{I}_L\right) C}$$

Applying ohms law to the load impedance, removes one degree of freedom and gives 3.2

Equation 3.2 Transfer function only dependent on voltages.

$$\underline{H}\left(\underline{s}, \underline{V}_{out}\right) = \frac{\underline{V}_{out}}{\underline{V}_{ps}} = \frac{1}{1 + \underline{s}\frac{L\left(\underline{V}_{out}\right)}{R} + \underline{s}^2 L\left(\underline{V}_{out}\right) C}$$

with

Equation 3.3 Inductors dependence on signal level.

$$L = \frac{\oint\limits_S \mu_0 \vec{H}\left(\underline{V}_{out}\right) \delta\vec{A}}{\oint\limits_C \vec{H}\left(\underline{V}_{out}\right) \delta\vec{l}} + \frac{\oint\limits_S \mu_0 \vec{M}\left(\underline{V}_{out}\right) \delta\vec{A}}{\oint\limits_C \vec{H}\left(\underline{V}_{out}\right) \delta\vec{l}}$$

Taking into account, that Petersons Coefficients, which are describing the nonlinearity of the inductor, are a series of polynoms, also the transfer function can be modeled by a series of polynoms, which is done in 3.4 up to second order for one signal frequency with the fitting coefficients α, β and γ.

Equation 3.4 Second order fitting of transfer function.

$$\underline{H}\left(\underline{V}_{l}oad\right) = \alpha\underline{H}^{2} + \beta\underline{H} + \gamma$$

A quantitative representation of the distortion for a 6.665 kHz sinusoidal test signal is the difference between an undistorted and a distorted signal. The undistorted signal as reference is taken from the output voltage of the signal after passing a linear filter as reference. The difference of those two voltages are known as distortion residual and for the modeled inductors shown in figures 6 and 7 for first and second order fitting respectively.

From those signals the root means square (RMS)

Fig. 6 Distortion residual for first order fitting.

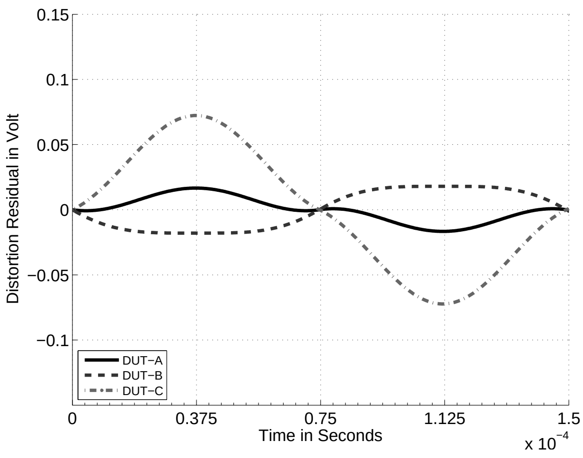

values can be numerically calculated and set in relation to the RMS of the desired signal according to the definition of total harmonic distortion (THD). This leads to the distortion figures, which are the ratio between the distortion residual and the signal before the filter, as shown in table 3.

4. SIMULATION

As has been described above, the inductors influence on distortion is only one of several influences.

Fig. 7 Distortion residual for second order fitting.

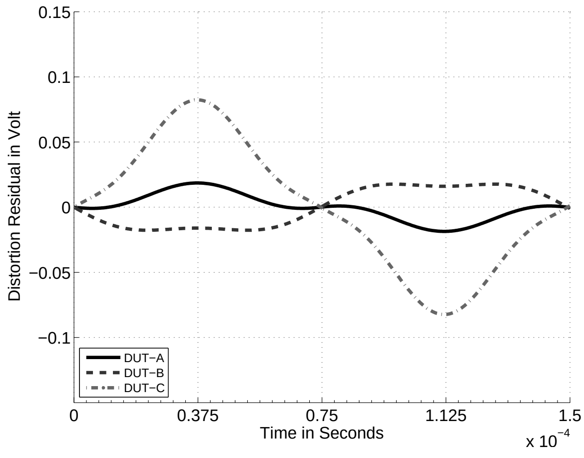

Table 3 Estimated total harmonic distortion (THD) for the modeled inductors.

	DUT-A	DUT-B	DUT-C
1st order fitting	0.034 %	0.053 %	0.165 %
2nd order fitting	0.036 %	0.053 %	0.171 %

Therefore the above model needs to enabled to connect with the other distortion mechanisms to reveal their interaction. This can be done with circuit analyzers like "GeckoCircuits". Therefore the nonlinear model of the above DUTs was simulated against their linear representations as shown in figure 8.
"GeckoCircuits" was chosen as simulation tool, because of its ability to directly deal with nonlinear passive components and its ability to process large simulation data very fast. The later property is relevant, because the distortion signal of an audio amplifier is generally very low compared to the signal. Therefore, both very precise simulation and large dynamical range of the simulator are required. In many software tools, this either leads to excess simulation time or large memory usage. "GeckoCircuits" requires neither one of them.
The simulation parameters and the duration of the simulation are given in table 4. The solver of this simulator takes all six modeled datapoints and interpolates the circuit behaviour linearly between those. The distortion residuals are shown in figures 9, 10 and 11. The simulated distortion numbers are given

Fig. 8 Simulated circuit with the three nonlinear models and their equivalent linear models.

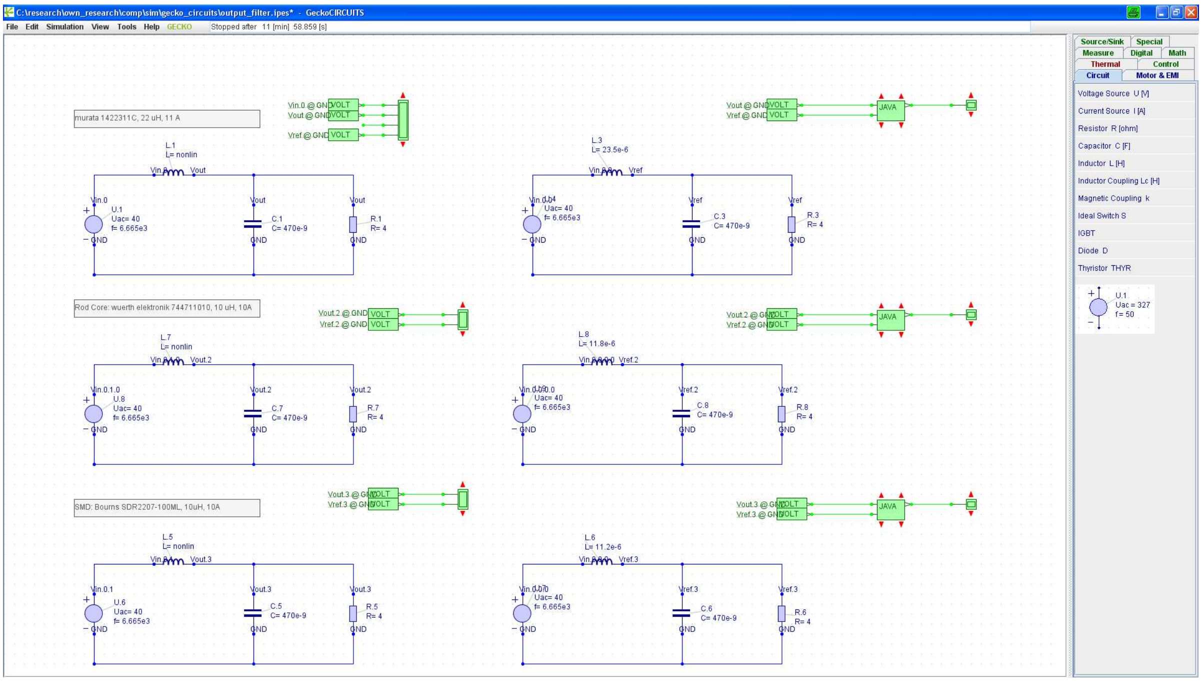

Table 4 Simulation parameters and duration.

start time	150 µs
time step	10 ps
stop time	300 µs
simulation time	≈ 12 min

in table 5.

The distortion is slightly higher here, however

Table 5 Estimated total harmonic distortion (THD) for the modeled inductors.

DUT-A	DUT-B	DUT-C
0.060 %	0.094 %	0.215 %

showing the same tendency as in the model above.

5. CONCLUSION

With distortion being a quantitative qualifier for an amplifier as starting point, the influences on this figure where revisited here. The focus within this study

Fig. 9 Simulated distortion residual based on the above model for DUT A. (x-axis: 150 µs . . . 300 µs; y-axis: −0.150 V . . . 0.15 V)

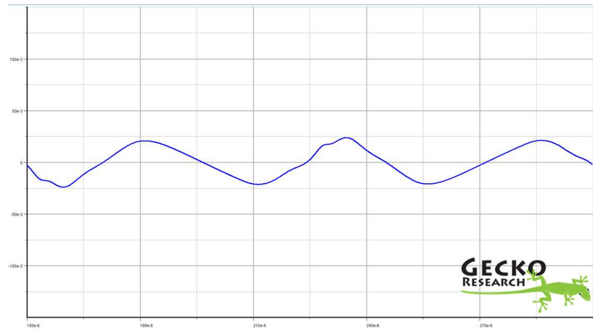

is on the output filters distortion and in particular the audio degradation induced by the inductor. After reviewing the physical reasons for the nonlinearity of both, the capacitor and the inductor, a procedure for modeling the nonlinearity of the inductor was shown. By fitting the transfer function of the output filter to this nonlinearity, an estimation on

Fig. 10 Simulated distortion residual based on the above model for DUT B. (x-axis: 150 µs . . . 300 µs; y-axis: −0.150 V . . . 0.15 V)

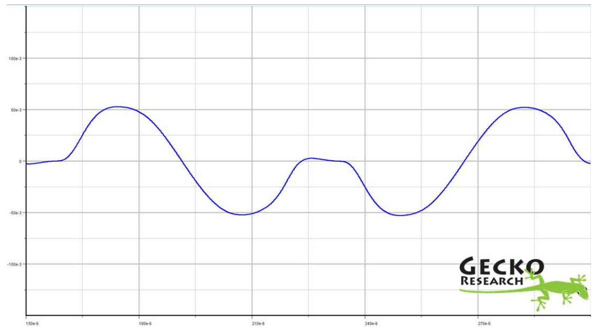

Fig. 11 Simulated distortion residual based on the above model for DUT C. (x-axis: 150 µs . . . 300 µs; y-axis: −0.150 V . . . 0.15 V)

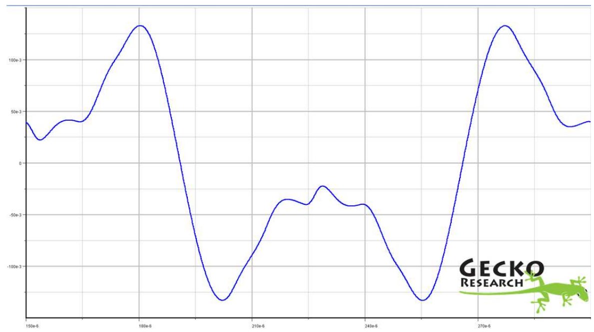

the amount of influence on the THD from the inductors linearity was derived. Finally the modeled component nonlinearity got applied to the filter in a circuit simulator to further enable the inclusion of the modeled details on system level.
As a rule of thumb the following mapping table 6 shall enable the design engineer of Class-D amplifiers to allow an estimation of THD, when the inductance drop at the rated current is the only known parameter — which is in some cases given in inductor datasheets.

Table 6 Mapping inductance droop to the caused THD as an approximated rule of thumb.

$\frac{\Delta L}{L_0}$	1 %	3 %	10 %
approximately expected THD	0.05 %	0.10 %	0.20 %

ACKNOWLEDGMENT

The authors want to thank Uwe Drofenik and Andreas Müsing from "Gecko Research" for his discussions and providing licenses for Gecko Circuits.

6. REFERENCES

[1] Audio Engineering Society Inc. AES standard method for digital audio engineering - Measurement of digital audio equipment. Standard AES17, AES Standards, March 1998.

[2] Douglas Self. *Audio Power Amplifier Design Handbook, Fourth Edition.* Newnes, 2006, ISBN: 978-0750680721.

[3] Pavel Pribyl. Spectral Representation of a PCM - PWM Digital Power Amplifier. *Audio Engineering Society Preprints*, 88th Convention(2920), February 1990.

[4] Floros, Andreas C.; Mourjopoulos, John N. Analytic Derivation of Audio PWM Signals and Spectra. *Audio Engineering Society Journal*, Vol. 46(7/8):621–633, July/August 1998.

[5] Goldberg, J.M.; Sandler, M.B. Noise Shaping and Pulse-Width Modulation for an All-Digital Audio Power Amplifier. *Audio Engineering Society Journal*, Vol. 39(6):446–460, June 1991.

[6] Floros, Andrew C.; Mourjopoulos, John N.; Tsoukalas, Dionysis E. Jither: The Effects of Jitter and Dither for 1-Bit Audio PWM Signals. *Audio Engineering Society Preprints*, 106th Convention(4956), April 1999.

[7] Hoyerby, M.C.W. Andersen, M.A.E. Carrier Distortion in Hysteretic Self-Oscillating Class-D Audio Power Amplifiers: Analysis and Optimization. *IEEE Transactions on Power Electronics*, 24(3):714–729, March 2009.

[8] Francois Koeslag, Toit Mouton. Accurate Characterization of Pulse Timing Errors in Class D Audio Amplifier Output Stages. *AES 37th International Conference*, (37th):72–81, August 2009.

[9] Harry F. Olson. *Acoustical Engineering*. Professional Audio Journals, Inc., 1991, ISBN: 91075297.

[10] Klippel, Wolfgang. Tutorial: Loudspeaker Nonlinearities-Causes, Parameters, Symptoms. *Audio Engineering Society Journal*, 54(10):907–939, October 2006.

[11] Knott, Arnold; Pfaffinger, Gerhard; Andersen, Michael A. E. On the Myth of Pulse Width Modulated Spectrum in Theory and Practice. *Audio Engineering Society Preprints*, 126th Convention(7799), May 2009.

[12] Polarization density. `http://en.wikipedia.org/wiki/Polarization_(electrostatics)`, August 2008.

[13] Sakabe, Y.; Kohno, Y.; Yamada, M.; Canner, J. Low Harmonic Distortion Ceramic-Multilayer Capacitor. *Proceedings of Electronic Components Conference*, (39th):202–205, May 1989.

[14] Lapshin, R.V. Analytical model for the approximation of hysteresis loop and its application to the scanning tunneling microscope. *Review of Scientific Instruments*, 66(9):4718–4730, September 1995.

[15] Rayleigh Lord. On the Behavior of Iron and Steel under the Operation of Feeble Magnetic Forces. *The Philosophical Magazine,*, XXV Notes on Electricity and Magnetism(5):225–245, March 1887.

[16] Peterson, E. Harmonic production in ferromagnetic materials at low frequencies and low flux densities. *Bell Systems Technical Journal*, 7:762–796, 1928.

[17] E. C. Snelling. *Soft ferrites: properties and applications*. Iliffe, Bristol, 1st edition, 1969, ISBN: 0592027902.

[18] Sagami. Power Inductors for Digital Amplifier. datasheet.

[19] Murata Power Solutions, Inc. Bobbin Type Inductors 1400Series. datasheet.

[20] Wuerth Electronik eiSos GmbH & Co.KG. . datasheet, August 2005.

[21] Bourns. SDR2207 Series - SMD Power Inductors. datasheet, October 2008.